# Formation of colloidal crystals of maghemite nanoparticles: Experimental and theoretical investigations

Anh-Tu Ngo, Salvatore Costanzo, Pierre-Antoine Albouy, Vincent Russier, Sawako Nakamae, Johannes Richardi, Isabelle Lisiecki

DOI: 10.1016/j.colsurfa.2018.10.021

# Formation of colloidal crystals of maghemite nanoparticles: Experimental and theoretical investigations

Anh-Tu Ngo,[1] Salvatore Costanzo,[1] Pierre-Antoine Albouy[2], Vincent Russier[3], Sawako Nakamae[4] Johannes Richardi[5*], Isabelle Lisiecki,[1*]

1-Sorbonne Université, CNRS, De la Molécule aux Nano-Objets: Réactivité, Interactions Spectroscopies, MONARIS, 75005, Paris France

2- Laboratoire de Physique des Solides, Université Paris-Sud, 91405 Orsay, France

3- ICMPE UMR 7182 CNRS and Université UPE, 2-8 rue Henri Dunant, 94320 Thiais, France.

4- CEA/DRF/IRAMIS/SPEC and CNRS UMR 3680, 91191 Gf sur Yvette, France

5- Sorbonne Université, CNRS, Laboratoire de Chimie Théorique, LCT, F. 75005 Paris, France

* Address correspondence to isabelle.lisiecki@upmc.fr and Johannes.Richardi@upmc.fr

**ABSTRACT:**

Novel colloidal crystals made of maghemite nanocrystals are fabricated by a co-evaporation method with ethanol. Thanks to a comprehensive characterization performed by grazing incidence small-angle X-ray scattering (GISAXS) and field emission gun scanning electron microscope (FEG-SEM), we show the first example of well-defined face-centered cubic (fcc) colloidal crystals. In order to obtain a clear picture of the crystal formation, the amount of ethanol in the solution is monitored using gas chromatography. In parallel, the interactions between the nanocrystals are calculated by statistical mechanics theory using solubility parameters. Theory predicts the formation of colloidal crystals at quite high amounts of ethanol around 15 %, in perfect agreement with experiment.

**KEYWORDS:** Maghemite nanoparticles, fcc colloidal crystallization, Solubility parameters, Flory theory of solvation

## 1. INTRODUCTION

The assembly of inorganic nanocrystals (NCs) in long-range ordered superlattices is a fascinating field of nanomaterials research.[1,2] These artificial solids exhibit new and enhanced collective properties (magnetic, mechanical, catalytic) arising from interactions between neighbouring NCs, making them very attractive for technological applications.[3-7] For engineering of advanced materials, it is crucial to perfectly control the assembly of NCs at microscopic scale. This task requires understanding what happens during the self-assembling of NCs into superlattices, which remains an open question. The homogeneous growth of colloidal crystals within a colloidal solution has emerged as a novel form of NC superlattices. Thanks to their perfect ordering at the microscopic scale and well-defined and tunable morphologies, these single supercrystals constitute ideal candidates not only to investigate their unique properties and the crystallization process resulting from the interactions between ligand-coated NCs. The

structural similarities between colloidal crystals and nanocrystals, their atomic counterpart, allow to improve our knowledge in crystallographic mechanisms at various scales.

In the literature, many colloidal crystals made of non-magnetic NCs have been reported, whereas only a few composed of magnetic NCs are published.[5, 8-11, 13-19] The main strategy used to grow these NC assemblies consists in a slow destabilization of the colloidal solution either by the diffusion technique of alcohol in the colloidal solution or by adding an excess of alkyl chains such as oleic acid. Their "crystallization" is always explained in terms of the reduction in the solubility of the NCs. However, a quantitative description for the conditions of the colloidal crystal formation is still missing. A better knowledge of these conditions is required to optimize the elaboration conditions such as the solvent in a controlled way.

In this paper, we use a classical method to fabricate colloidal crystals composed of maghemite NCs: an NC solution in hexane is co-evaporated in the presence of a second beaker containing ethanol so as to allow ethanol to progressively diffuse into hexane. Here the colloidal crystals are distinguished from the super lattices as resulting from a homogeneous growth process and characterized by an overall size in the few micrometers range.

Thanks to a novel setup, the alcohol transfer into the hexane is accurately controlled. The colloidal crystals are characterized by SEM, FEG-SEM and GISAXS techniques. The evolution of ethanol contents in both beakers is measured using gas chromatography. In parallel, the interaction between NCs as a function of the solvent is calculated. These calculations are based on the Flory theory using Hansen solubility parameters.[20] Thus, we obtain a coherent picture of the mechanisms underlying the superlattice formation. The proportion of ethanol into NC solution increases up to 15 %, value for which the calculations predict attractive interactions between the NCs. To the best of our knowledge, we propose, for the first time, a quantitative explanation for the colloidal crystal growth induced by the slow ethanol diffusion in the colloidal solution based on the solvent-mediated interactions between NCs. In addition,

this study highlights a novel class of colloidal crystals made of maghemite NCs with an unprecedented superstructure characterization, here, fcc.

## 2. EXPERIMENTAL METHODS

### Products

All materials were used as purchased without further purification. Iron chloride ($FeCl_3.6H_2O$, 99%, Prolabo) sodium dodecanoate ($CH_3(CH_2)_{10}COONa$, 97%, TCI), dodecanoic acid ($CH_3(CH_2)_{10}COOH$, 99.5%, Acros) and 1-octadecene (90%, Sigma Aldrich).

### Synthesis of Dodecanoic Acid Coated 12.7 nm γ-$Fe_2O_3$ Nanocrystals

12.7 nm γ-$Fe_2O_3$ NCs having a low size-dispersion (5 %) are synthesized by thermal-decomposition of iron-dodecanoate complex.[21] Dodecanoic acid and iron-dodecanoate complex are dissolved in 1-octadecene. This mixture is heated to the boiling point of 1-octadecene under stirring and is refluxed for 30 min and then cooled to room temperature. A black gel is formed and washed with a large excess of ethanol to collect the NCs. The NCs are dispersed in hexane. For the TEM study, some drops of the colloidal solution are deposited on an amorphous carbon coated TEM grid. The average diameter and the polydispersity are determined from more than 700 particles. The electron diffraction spots in the measurements of nanocrystals are indexed to the maghemite structure (γ-$Fe_2O_3$).

### Synthesis of Colloidal Crystals made of 12.7 nm- γ-$Fe_2O_3$ NCs

Colloidal crystals made of 12.7 nm γ-$Fe_2O_3$ NCs are produced as follows: 200 μL of a colloidal solution in hexane containing 0.03 % by weight of nanocrystals is added to a vertically positioned glass beaker (*beaker 1*), 1.5 cm in height and 1 cm in diameter, at the bottom of which a silicon wafer (5 x 5 $mm^2$) is positioned horizontally. Another beaker (*beaker 2*) having the same size is filled with 800 μL of ethanol and positioned next to the previous one. The two beakers remain opened and are positioned inside a third one, 4.2 cm in length and 2.5 cm in diameter, which is sealed and left at room temperature for

approximately 12 h. After total evaporation of the solvent in beaker 1, the as-prepared samples are investigated by SEM, SEM-FEG and SAXS techniques.

**Transmission Electron Microscopy (TEM)**

TEM study is performed using a JEOL JEM-1011 microscope at 100 kV.

**Scanning Electron Microscopy (SEM)**

SEM studies are performed using a scanning electron microscope (SEM, JEOL 5510 LV) and a field emission gun scanning electron microscope (FEG-SEM, Hitachi Su-70).

**Grazing Incidence Small-Angle X-Ray Diffraction (GISAXS)**

Grazing incidence small-angle X-ray scattering (GISAXS) measurements were carried out using a rotating anode generator operated with a small size focus (copper anode; focus size 0.2 mm x 0.2 mm; 50kV, 30mA). The optics consisted of two parabolic multilayer graded mirrors in KB geometry providing a parallel monochromatic beam. The sample was mounted on a rotating stage and the diffraction patterns were recorded on photo-stimulable imaging plates. Vacuum pipes are inserted between the sample and the imaging plate to reduce air scattering. A single GISAXS measurement probes a section, several micrometers wide, from one edge of the substrate to the other.

**Gas Chromatography-Flame Ionization Detection (GC-FID)**

The quantification of ethanol was performed using GC-FID apparatus (Thermo Quest Trace GC).[22] The column used was a ZB Wax plus (Phenomenex – 30 m x 0.25 mm ID x 0.25 μm df). The initial column temperature was set to 60 °C and programmed to increase at a rate of 20 °C/min to 130 °C. The injector and the detector temperatures were set to 250 °C. Hydrogen was used as carrier gas giving a column flow of 1.6 mL/min. 1 μl of solution was injected in a split/splitless injector: split mode (split ratio 10). The solvent used was dodecane.

**Theory: Interaction Model**

The model proposed and described in detail in the references 23 and 24 was used using the code NanoForceG. The interaction energy between nanocrystals are calculated as a sum of the van-der-Waals attraction between the metallic cores of the particles, the free energy of mixing of the ligands, the elastic compression of the ligands, and magnetic interaction between the cores. The interaction parameter $\chi_{12}$ between the solvent 1 and the ligand 2 is calculated from the usual equations[23]: $\chi_{12} = V_s A_{1,2} / R T + \beta$ with $A_{1,2} = (\delta_{D2} - \delta_{D1})^2+0.25(\delta_{P2} - \delta_{P1})^2+0.25 (\delta_{H2} - \delta_{H1})^2$. $\delta_D$, $\delta_P$ and $\delta_H$ are the Hansen solubility parameters for the dispersion, polar and hydrogen bonding interactions, respectively. For $\beta$ the generally accepted average value near 0.34 is used.[23] For other systems we have observed that this factor is essential to obtain results in agreement with the experiments. The magnetic dipole moments are calculated from the saturation magnetization (maghemite nanoparticles: $3.75\ 10^5\ Am^{-1}$). The molecular volumes and the solubility parameters published in reference 23 are used to describe the ligand and the solvents. For the dodecanoic acid, the counter length is estimated at 1.78 nm following reference 25. The average core surface covered by one ligand is estimated from the head group size at (16 $Å^2$) which is a typical value found in nanocrystals. The Hamaker constant for the van der Waals interaction for the maghemite nanocrystals is taken from reference 26 considering the solvent (maghemite: $10.0\ 10^{-20}$ J).

To estimate the influence of the presence of ethanol in the solvent hexane on the nanoparticle interactions, we calculated an average molecular volume and solubility parameter for the solvent ($V_s$ = f(hexane) $V_s$(hexane) + f(ethanol) $V_s$(ethanol) and ($\delta_s$ = f(hexane) $\delta_s$(hexane) + f(ethanol) $\delta_s$(ethanol)). f(hexane) and f(ethanol) is the molar amount of hexane or ethanol in the solvent.

## 3. RESULTS AND DISCUSSION

### 3.1. Experimental investigation of the colloidal crystals of γ-$Fe_2O_3$ NCs

γ-$Fe_2O_3$ nanocrystals of 12.7 nm in diameter were synthesized by thermal-decomposition of iron-dodecanoate complex and dispersed into hexane. The as-prepared solution was added into a beaker and

evaporated in the presence of a second beaker with ethanol. After a total evaporation of the solvent the samples are investigated by SEM, FEG-SEM and GISAXS techniques.

The SEM study performed on the sample made with dodecanoic acid coated 12.7 nm $\gamma$-$Fe_2O_3$ NCs characterized by a low size distribution of 5% (Inset Figure 1a), shows an extensive production of assemblies reaching sizes up to 2.4 of micrometers (Figure 1a).

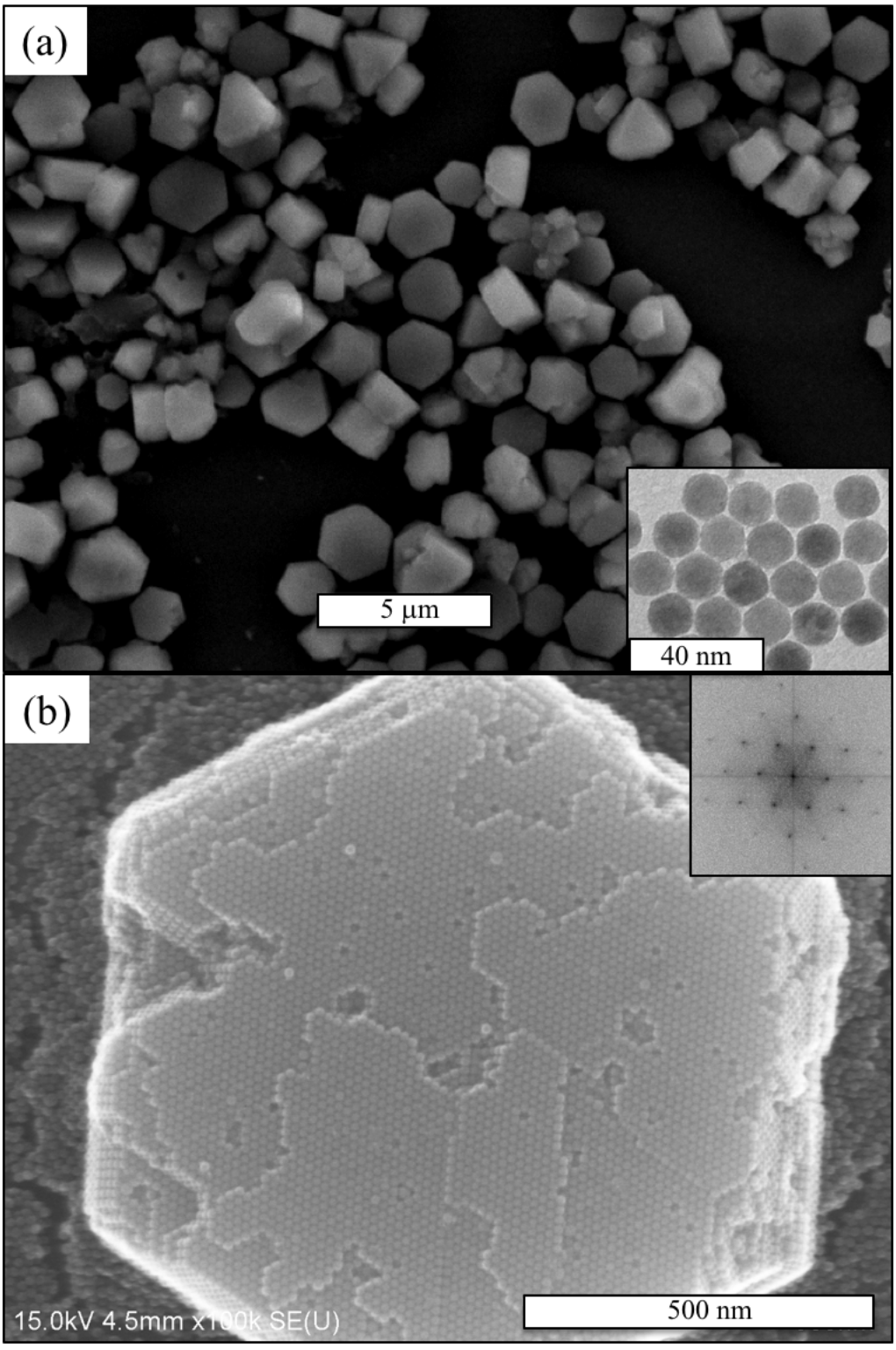


**Figure 1.** (a) SEM images of colloidal crystals made of 12.7 nm γ-$Fe_2O_3$ NCs. The inset is a TEM image of γ-$Fe_2O_3$ NCs. (b) FEG-SEM image of a colloidal crystal made of 12.7 nm γ-$Fe_2O_3$ NCs. The inset is the Fast Fourier transform of the colloidal crystal.

Various morphologies, *i.e.*, triangles, truncated triangles and hexagons, are obtained. Whatever the morphology, these assemblies all exhibit regular facets, clear edges and sharp corners. This geometrical trend is consistent with the formation of ordered assemblies of NCs, in solution [9-12] or in the Tagish Lake meteorite.[13] The average frequencies of triangles, truncated triangles and hexagons obtained with more than 600 single objects are 14 %, 37 % and 49 %, respectively. Focusing on one hexagon, a high-resolution SEM image shows a regular stacking of NCs on the top layer of the assembly, indicating the existence of a likely long-range ordered 3D assembly (Figure 1b). A six-fold symmetry and 2D hexagonal packing are observed on the top layer of the assembly and confirmed by the Fast Fourier transform (FFT) pattern (Inset Figure 1b). This is compatible with either the hexagonal compact packing (hcp) or the face-centered cubic (fcc) 3D structure. Similarly, to their atomic counterparts, terraces and steps are visible on the edges of the objects. The mean thickness of these isolated assemblies is found around 760 nm. To determine the 3D structure of these single assemblies, grazing small-angle X-ray diffraction is performed. The diffraction pattern (Figure 2) is typical for an oriented powder, where domains have an fcc structure and are mostly oriented with the [111] perpendicular to the substrate.[27] The weak continuous ring observed on the diffraction pattern, is due to the randomly oriented colloidal crystals, clearly visible in the SEM image showed in Figure 1A. The modulus of the q-vector associated to the (111) reflection is $q_{111} = 2\pi\sqrt{3}/a$ where $a$ is the cubic parameter. The value deduced from the X-ray pattern is $q_{111}$= 0.505 nm$^{-1}$, that leads to $a$ = 21.54 nm and an inter-particle distance $D_{c\text{-}c}$ = 15.2 nm. Taking into account the average NC diameter of 12.7 nm, we find the inter-particle gap of 2.5 nm. Reflection-like spots in non-equatorial position are well-defined, which indicates the absence of stacking faults.

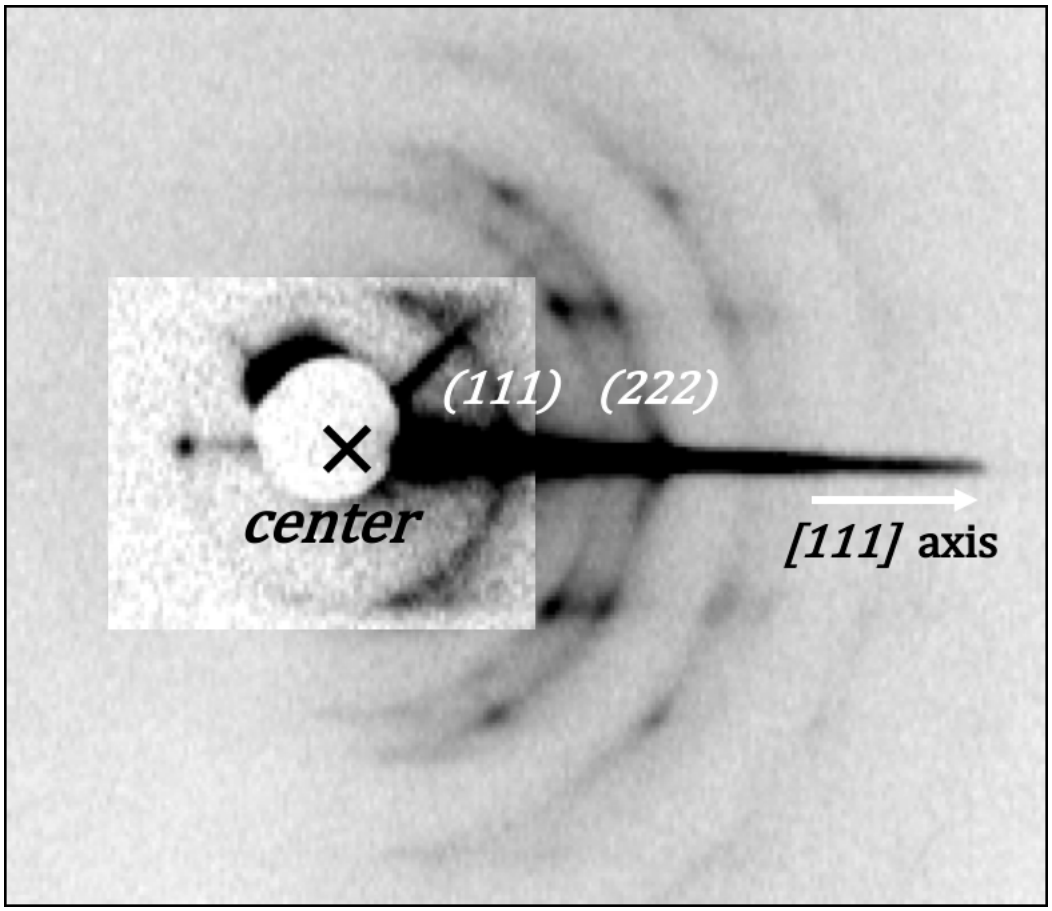


**Figure 2.** SAXRD of the colloidal crystals made of 12.7 nm γ-$Fe_2O_3$ NCs shown in Figure 1

### 3.2. Experimental Monitoring of the Formation of the Colloidal Crystals of γ-$Fe_2O_3$

The slow destabilization of the colloidal solution by the controlled diffusion of alcohol is well known to promote the formation of colloidal crystals. In order to quantitatively follow this process, two open glass beakers, one containing 200 μl ($V_1$) of the colloidal solution of NCs with the silicon wafer placed at the bottom, and the other with 800 μl ($V_2$) of ethanol, are placed in a closed bottle (Figure 3a). The reduced height is defined as the ratio h(t) / h(t=0) where h(t) is the height of the solution at time t. Evolution of the reduced height of ethanol and colloidal solution of NCs in hexane at different times are compared during the entire duration of the experiment. As shown in the graphic (Figure 3c), the reduced height of ethanol ($V_2$) increases by 18% after 350 min and remains quite stable until the end of the deposition process. Besides, the reduced height of the colloidal solution in hexane ($V_1$) decreases, until the near total

evaporation of the solution, occurring after 480 min. The evaporation process starts from the center toward the edges of the substrate. It is observed that after 270 min (Figure 3b), a large part from the center of the substrate is no longer immersed in the beaker containing the NCs solution. After 350 min, the substrate is totally free of the colloidal solution.

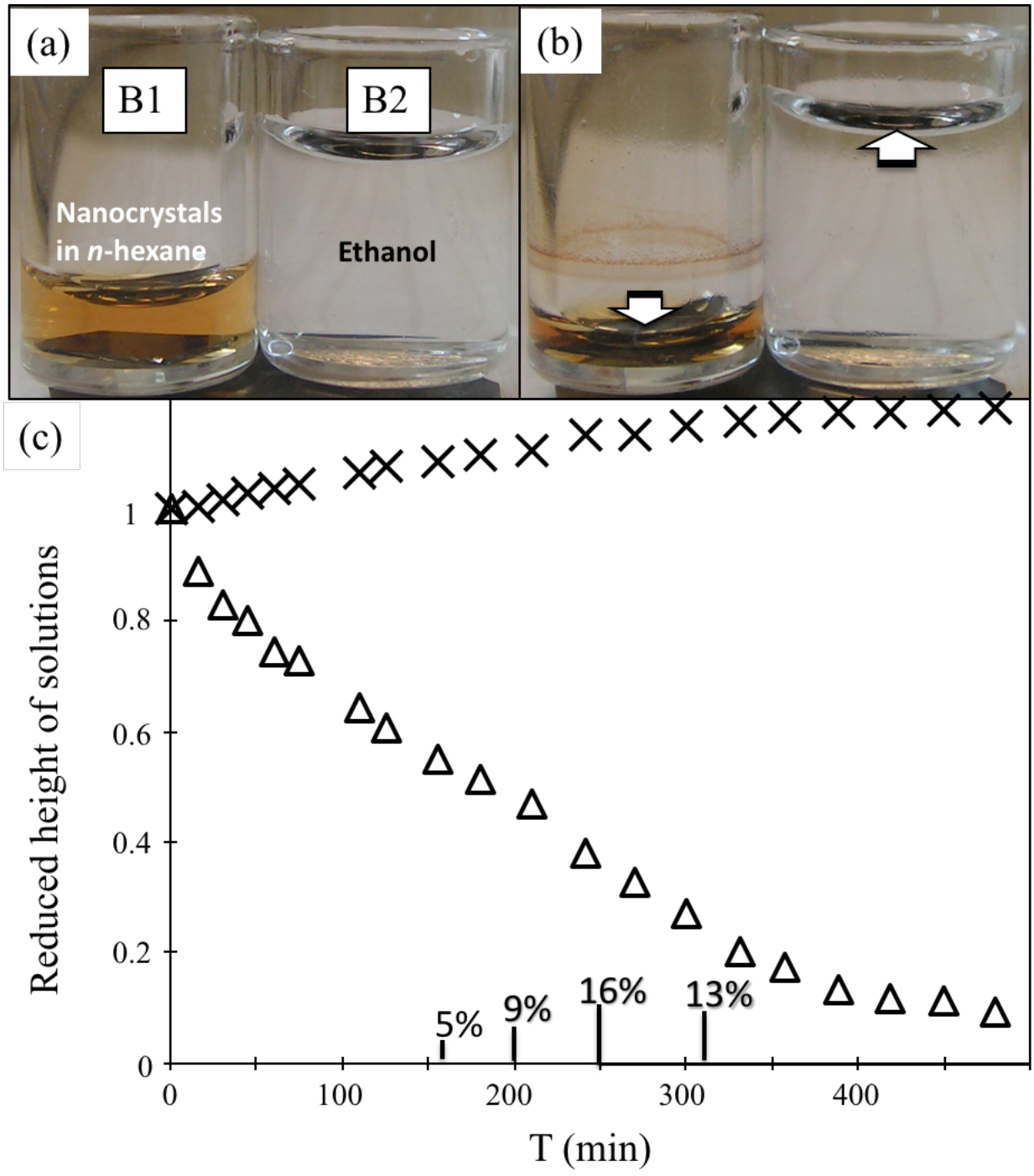




11

**Figure 3.** Selected photographs of the beakers at initial state (a) and after 270 min (b) during the evaporation process. (c) Evolution of the reduced height on the beakers for solutions of nanocrystals in hexane (B1, "**Δ**") and ethanol (B2, "**X**") at different times. The vertical bars indicate the percentage of ethanol in the beaker containing nanocrystals in hexane at selected times obtained with Gas Chromatography-Flame Ionization detection.

The evolution of the relative liquid heights in the 2 beakers results from a complex process. Nevertheless from the Hertz-Knudsed law, and using the values of the saturated vapor pressure at 25 °C on one hand (7.927 kPA (ethanol) and 20.265 kPa (hexane)), and the molar masses on the other hand (46 g/mol (ethanol) and 86 g/mol (hexane)), and the molar volumes ($v_m$ = 58.5 $cm^3$/mol (ethanol), 130 $cm^3$/mol (hexane)), one can estimate a volumic evaporation rate about 8 times higher for hexane than for ethanol if we neglect the partial pressures of both solvents in the vapor surrounding the beakers (the volumic evaporation rate is then proportional to $v_m\sqrt{(M/kT)}p_s$).[28] From this estimation we can conclude that the total volume of hexane is evaporated before a significant part of the initial volume of ethanol. However, the amount of ethanol dissolved in the beaker with the NC solution is unknown. The following theory will show that this amount is central to explain the formation of colloidal crystals. The quantification of ethanol was performed by Gas chromatography-flame ionization detection (GC-FID). The ethanol percentages in hexane are found equal to 5, 9, 16 and 13 % after 160, 200, 250 and 310 min, respectively.

### 3.3. Theoretical Investigation of Formation of Colloidal Crystals of γ-$Fe_2O_3$ NCs

In order to understand the homogeneous nucleation of colloidal crystals, we calculated the interaction between the nanocrystals. Recent works have shown that the solvent markedly influences these interactions.[23,24,29] We used the model proposed and described in detail in the references 23 and 24 using the code NanoForceG. It assumes that the interaction potential is defined as the sum of the van-der-Waals attraction between the metallic cores of the particles, the free energy of mixing of the ligands, and the

elastic compression of the ligands. To take into account the magnetic interactions, a Keesom term was added.[26] The details of the computations are given in the method section.

In Figure 4, the interaction potential between the nanocrystals is shown as a function of the amount of ethanol in hexane. In previous simulations it has been observed that when a threshold of -3 kT is reached for the interaction between nanocrystals, a homogeneous nucleation occurs observed presently.[23,24] It is explained by the fact that the attraction between the nanocrystals becomes strong enough to induce self-assembly. Figure 4 shows that the amount of ethanol has to be quite large (> 15%) to observe a homogeneous nucleation.

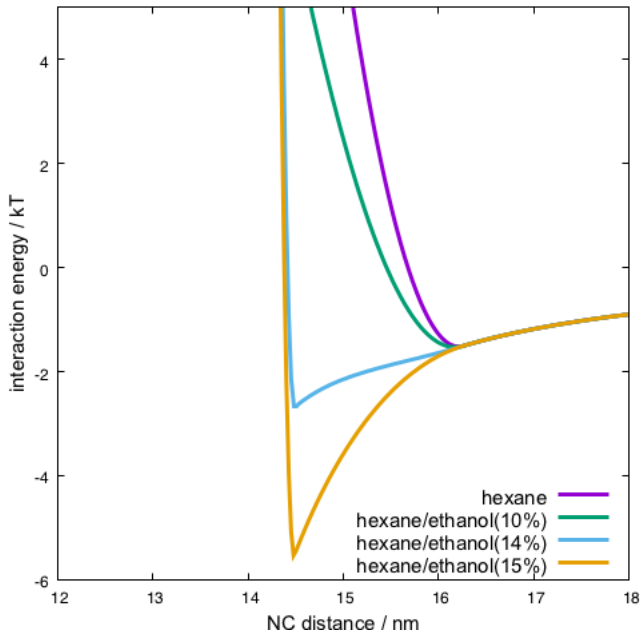


**Figure 4.** Interaction energy between two dodecanoic acid coated γ-$Fe_2O_3$ NCs of 12.7 nm as a function of the nanoparticle distance for different amounts of ethanol in hexane.

The measurement of ethanol in hexane during the evaporation by gas chromatography-flame shows that such a high percentage of ethanol (>15%) is actually reached at around 250 min (see Figure 4). This shows that, from a theoretical point of view, the experimental conditions permit a homogeneous nucleation. The formation of colloidal crystals is explained by the solvent mediated ligand interaction induced by the "bad" solvent ethanol. This is mainly due to the free energy term of mixing, while the

van-der-Waals and magnetic interactions only play minor roles. Indeed, the solubility parameters for ethanol used to calculate the energy of mixing are significantly higher than for dodecane. This means that the ethanol molecules prefer to stick together and avoid the contact with the dodecanoic ligands, which leads to an attraction between the nanoparticles.

This leads to the following description of the mechanism of colloidal growth formation. During the co-evaporation, the concentration of ethanol in the nanocrystal solution increases to reach a threshold of 15 %. From this threshold, colloidal crystals form due to homogeneous nucleation induced by the attraction between the nanocrystals predicted by the theory.

## 4. CONCLUSIONS

To the best of our knowledge, we show the crystallization of novel colloidal crystals, made of 12.7 nm nanocrystals of maghemite, obtained by a co-evaporation experiment with ethanol. The perfectly facetted crystals, are characterized by various shapes i.e., triangles (14 %), truncated triangles (37 %) and hexagons (49 %). A comprehensive characterization performed by GISAXS and FEG-SEM, evidences for the first time, perfectly ordered superstructures, here, face-centered cubic. Experiment and theory give the following picture for the colloidal crystal formation. When a proportion in ethanol into the NCs solution of ca. 15% is reached, interactions between NCs become attractive, leading to the formation of the colloidal crystals. The theory enables us to predict the best conditions and solvents for co-evaporation experiments. For instance, in good agreement with the experiment theory does predict no formation of colloidal crystals, when ethanol is replaced by toluene or water. In the first case toluene is not able to induce attraction between the NCs. The absence of colloidal crystals for water is explained by the fact that water is not soluble in hexane.

**ACKNOWLEDGEMENTS**

FEG-SEM instrumentation was facilited by the Institut des Matériaux de Paris Centre (IMPC FR2482) and was funded by Sorbonne Université, CNRS and by the C'Nano projects of the Région Ile-de-France. The authors thank Isabelle Pellerin, Romain Descamps and Sophie Rochut for helpful assistance and for fruitful discussions with Gas Chromatography-Flame Ionization Detection (GC-FID) (Plateforme de Chimie Analytique, Physique et Spectroscopie, Sorbonne Université, F-75005 Paris, France.

The research leading to these results has been supported by a grant ANR-CE08-007 from the ANR French Agency

**REFERENCES**

(1) Z. Nie, A. Petukhova, E. Kumacheva, Properties and emerging applications of self-assembled structures made from inorganic nanocrystals, Nat. Nanotechnol. 5 (2010) 15-25.

(2) H. Zhang, E. W. Edwards, D. Wang, H. Möhwald, Directing the self-assembly of nanocrystals beyond colloidal crystallization, Phys. Chem. Chem. Phys. 2006, 8, 3288-3299.

(3) I, Lisiecki, M. P. Pileni, Ordering at various scales: Magnetic Nanocrystals, J. Phys. Chem. C. 116 (2012) 3-14.

(4) A, Dreyer, A. Feld, A. Kornowski, E. D. Yilmaz, H. Noei, A. Meyer, T. Krekeler, C. Jiao, A. Stierle, V. Abetz, H. Weller, Organically linked iron oxide nanoparticle supercrystals with exceptional isotropic mechanical properties, Nature Materials 15 (2016) 522-528.

(5) J. Park, E. Kang, S. U. Son, H. M. Park, M. K. Lee, J. Kim, K. W. Kim, H. J. Noh, J. H. Park, C. J. Bae, J. G. Park, T. Hyeon, Monodisperse Nanoparticle of Ni and NiO: Synthesis, Characterization, Self-Assembled Superlattices, and Catalytic Applications in the Suzuki Coupling Reaction, Adv. Mater. 17 (2005) 429-434.

(6) R. Y. Wang, J. P. Feser, J. S. Lee, D. V. Talapin, R. Segalman, A. Majundar, Enhanced Thermopower in PbSe Nanocrystal Quantum Dot Superlattices, Nanolett. 8 (2008) 2283-2288.

(7) A. Çolak, J. Wei, I. Arfaoui, M. P. Pileni, Coating agent-induced mechanical behavior of 3D self-assembled nanocrystals, Phys. Chem. Chem. Phys. 2017, 19, 23887-23897

(8) C. H. Liao, Y. S. Lin, K. Chanda, Y. F. Song, M. H. Huang, Formation of Diverse Supercrystals from Self-Assembly of a variety of polyhedral gold nanocrystals, J. Am. Chem. Soc. 135 (2013) 2684-2693.

(9) D. V. Talapin, E. V. Shevchenko, A. Kornowski, N. Gaponik, M. Haase, A. L. Rogach, H. A New Approach to Crystallization of CdSe Nanoparticles in Ordered Three-Dimensional Superlattices, Adv. Mater. 13 (2001) 1868−71.

(10) K. Ouhenia-Ouadahi, A. Andrieux-Ledier, J. Richardi, P-A. Albouy, P. Beaunier, P. Sutter, E. Eli Sutter, A. Courty, Tuning the Growth Mode of 3D Silver Nanocrystal Superlattices by Triphenylphosphine, Chem. Mater. 28 (2016) 4380-4389.

(11) E. S. Shibu, M.A.H. Muhammed, K. Kimura, T. Pradeep, Fluorescent Superlattices of gold Nanopartcicles: A New Class of Functional Materials, Nano Res. 2 (2009) 220-234.

(12) N. Goubet, H. Portales, C. Yang, I. Arfaoui, P. A. Albouy, A. Mermet, M. P. Pileni, Simultaneous Growths of Gold Colloidal Crystals, J. Am. Chem. Soc. 2011,134, 3714-3719.

(13) J. Nozawa, K. Tsukamoto, W. Willem van Enckevort, T. Nakamura, Y. Kimura, H, Miura, H. Hisao Satoh, K. Ken Nagashima, M. Konoto, Magnetite 3D Colloidal Crystals Formed in the Early Solar System 4.6 Billion Years Ago, J. Am. Chem. Soc. 133 (2011) 8782-8785.

(14) A. L. Rogach, D. V. Talapin, E.V. Shevchenko, A. Kornowski, M. Haase, H. Weller, Organization of Matter on Different Size Scales: Monodisperse Nanocrystals and Their Superstructures. Adv. Funct. Mater. 12 (2002) 653-664.

(15) E. Shevchenko, D. Talapin, A. Kornowski, F. Wiekhorst, J. Kotzler, M. Haase, A. Rogach, H. Weller, Colloidal Crystals of Monodisperse FePt Nanoparticles Grown by a Three-Layer Technique of Controlled Oversaturation, Adv. Mater. 14 (2002) 287−289.

(16) N. Yang, Z. Yang, M. Held, P. Bonville, P.A. Albouy, R. Lévy, M.P. Pileni, Dispersion of Hydrophobic Co supracrystal in Aqueous Solution, ACS Nano, 10 (2016) 2277-2286.

(17) L. r. Meng, W. Chen, Y. Tan, L. Zou, C. Chen, H. Zhou, Q. Peng, Y. Li, $Fe_3O_4$ Octahedral Colloidal Crystals, Nano Res. 4 (2011) 370-375.

(18) O. Kasyutich, D. Tatchev, A. Hoell, F. Ogrin, C. Dewhurst, W. Schwarzacher, Small angle x-ray and neutron scattering Study of Disordered and Three Dimensional-Ordered Magnetic Protein Array, J. Appl. Phys. 105 (2009) 07B528-1-3.

(19) F. Dumestre, B. Chaudret, C. Amiens, P. Renaud, P. Fejes, Superlattices of Iron Nanocubes Synthesized from $Fe[N(SiMe_3)_2]_2$, Science, 303 (2004) 821-824.

(20) C.M. Hansen in *Hansen's solubility parameters: A user's Handbook*, CRC Press, Boca Raton, 2000.

(21) A. T. Ngo, J. Richardi, M. P. Pileni, Crack patterns in superlattices made of maghemite nanocrystals, Phys. Chem. Chem. Phys. 15 (2013) 10666-10672.

(22) A. O Cherif, M. B. Messaouda, B, Kaabi, I. Pellerin, S. Boukhchina, H. Kallel, C. Pepe, C. Characteristics and pathways of bioactive 4-desmethylsterols, triterpene alcohols and 4α-monomethylsterols, from developing Tunisian cultivars and wild peanut (Arachis hypogaea L.), Plant Physiology and Biochemistry. 49 (2011) 774-781.

(23) N. Goubet, J. Richardi, P. A. Albouy, M. P. Pileni, How to Predict the Growth Mechanism of Supracrystals from Gold Nanocrystals, J. Phys. Chem. Lett. 2 (2011) 417–422.

(24) N. Goubet, J. Richardi, P. A. Albouy, M. P. Pileni, Which Forces Control Supracrystal Nucleation in Organic Media? Adv. Funct. Mater. 21 (2011) 2693–2704

(25) C. D. Bain, E. B. Troughton, Y. T. Tao, J. Evall, G.M . Whitesides, R. G. Nuzzo, Formation of monolayer films by the spotaneous assembly of organic thiols from solution onto gold, J. Am. Chem. Soc. 111 (1989) 321-335.

(26) J. Israelachvili in *Intermolecular and surface Forces, 3rd edition*. Academic Press, 2011, Burlington, ISBN: 978- 0-12-391927-4.

(27) I. Lisiecki, P. A. Albouy, M. P. Pileni, Face-Centered-Cubic "Supracrystals" of Cobalt Nanocrystals, Adv. Mater. 15 (2003) 712-716.

(28) T. Ytrehus, S. Østmo, Kinetic theory approach to interphase process, Int. J. Multiphase Flow. 22 (1996) 133-155

(29) K. Z. Milowska and J. K. Stolarczyk, Role of ligand–ligand *vs.* core–core interactions in gold nanoclusters, Phys. Chem. Chem. Phys. 18 (2016) 12716-12724.